Atmos. Chem. Phys., 12, 9581–9592, 2012
www.atmos-chem-phys.net/12/9581/2012/
doi:10.5194/acp-12-9581-2012

Atmospheric Chemistry and Physics

Atmospheric impacts on climatic variability of surface incident solar radiation

K. C. Wang[1], R. E. Dickinson[2], M. Wild[3], and S. Liang[4]

[1]State Key Laboratory of Earth Surface Processes and Resource Ecology, College of Global Change and Earth System Science, Beijing Normal University, Beijing, 100875, Beijing, China
[2]Department of Geological Sciences, The University of Texas at Austin, Austin, TX 78712, USA
[3]Institute for Atmospheric and Climate Science, ETH Zürich, 8092 Zürich, Switzerland
[4]Department of Geography, University of Maryland, College Park, MD 20742, USA

Correspondence to: K. C. Wang (kcwang@bnu.edu.cn)

Received: 20 April 2012 – Published in Atmos. Chem. Phys. Discuss.: 6 June 2012
Revised: 21 September 2012 – Accepted: 5 October 2012 – Published: 22 October 2012

Abstract. The Earth's climate is driven by surface incident solar radiation (R_s). Direct measurements have shown that R_s has undergone significant decadal variations. However, a large fraction of the global land surface is not covered by these observations. Satellite-derived R_s has a good global coverage but is of low accuracy in its depiction of decadal variability. This paper shows that daily to decadal variations of R_s, from both aerosols and cloud properties, can be accurately estimated using globally available measurements of Sunshine Duration (SunDu). In particular, SunDu shows that since the late 1980's R_s has brightened over Europe due to decreases in aerosols but dimmed over China due to their increases. We found that variation of cloud cover determines R_s at a monthly scale but that aerosols determine the variability of R_s at a decadal time scale, in particular, over Europe and China. Because of its global availability and long-term history, SunDu can provide an accurate and continuous proxy record of R_s, filling in values for the blank areas that are not covered by direct measurements. Compared to its direct measurement, R_s from SunDu appears to be less sensitive to instrument replacement and calibration, and shows that the widely reported sharp increase in R_s during the early 1990s in China was a result of instrument replacement. By merging direct measurements collected by Global Energy Budget Archive with those derived from SunDu, we obtained a good coverage of R_s over the Northern Hemisphere. From this data, the average increase of R_s from 1982 to 2008 is estimated to be 0.87 W m^{-2} per decade.

1 Introduction

Solar radiation drives the Earth's climate system. The amount that is incident at the surface, denoted R_s and measured by a surface network of radiometers, has been shown to undergo significant decadal variations (Gilgen et al., 1998; Liepert, 2002; Long et al., 2009; Ohmura, 2009; Stanhill and Cohen, 2001; Wild et al., 2005). In particular, direct measurements with limited coverage show that the dimming trend of R_s that occurred up to the late 1980's reversed to a widespread brightening after that (Wild, 2009; Wild et al., 2005). Satellite-derived R_s (Pinker et al., 2005) has a better spatial coverage but may have spurious variability resulting from changes of satellites, their sensor calibration, and undetected low clouds (Evan et al., 2007). It also can be biased by its exclusion of variations of tropospheric aerosols over land (Wang et al., 2009). These changes in atmospheric aerosols contributed to the observed decadal variation in R_s over Europe (Norris and Wild, 2007) and Asia (Norris and Wild, 2009). It is not surprising that the decadal variations in satellite-derived R_s have been substantially different from those of radiometer measurements at the surface (Hayasaka et al., 2006; Xia et al., 2006).

This paper improves the surface-based global coverage of estimates of R_s by using Sunshine Duration (SunDu), a measurement initiated 150 yr ago (Sanchez-Lorenzo and Wild, 2012), which records the time during a day that the direct solar irradiance exceeds 120 W m^{-2}. It is one of the oldest and most robust measurements related to radiation (Wild, 2009).

Worldwide direct R_s measurements only began in the late 1950's. SunDu observations provide a globally-distributed proxy record of R_s at both urban and rural sites with a much higher density than that of the direct measurements as obtained from the of Global Energy Budget Archive (GEBA) (Gilgen et al., 1998). Consequently, these observations allow us to fill in the blank areas of the GEBA coverage.

Several previous studies have established good correlations between SunDu and R_s (Essa and Etman, 2004; Hoyt, 1977; Sanchez-Lorenzo et al., 2009; Stanhill and Cohen, 2005). SunDu has been regarded as a measure of cloud cover. However, studies have shown that aerosols can also reduce SunDu (Horseman et al., 2008; Kaiser and Qian, 2002; Raschke et al., 2006; Sanchez-Lorenzo et al., 2008, 2009; Tang et al., 2011). This paper further demonstrates that SunDu can be used to estimate R_s globally with sufficient accuracy to establish its year-to-year variations. It then examines the year to decadal variations of R_s and their potential causes.

2 Data

SunDu records the time during a day that direct solar beam irradiance exceeds 120 W m^{-2}. It was initiated 150 yr ago and is one of the oldest and most robust measurements related to radiation (Wild, 2009). In 1962 the Campbell-Stokes sunshine recorder was recommended as the reference SunDu sensor by the World Meteorological Organization (WMO) in order to homogenize the data of the worldwide network for SunDu (WMO, 2008).

One advantage of SunDu is that the impact of sensor replacement on SunDu measurement is rather small. Three different types of sunshine duration recorders were used from 1888 to 1987 in the USA (Stanhill and Cohen, 2005): first, the Jordan photographic recorder from 1888 to 1907; second, the Maring-Marvin thermometric sunshine recorder from 1893 to the mid-1960s; and third, the Foster photoelectric Sun Switch (beginning in 1953). Replacement of the recording method has been shown to have a negligible effect on the annual SunDu (Stanhill and Cohen, 2005).

The World Meteorological Organization (WMO, 2008) requires that hours of sunshine should be measured with an uncertainty of ± 0.1 h and a resolution of 0.1 h. There has been no standardized method to calibrate SunDu detectors. For outdoor calibration, the pyrheliometric method was recommended as a reference method, which detects the transition of direct solar irradiance through the 120 W m^{-2} threshold (WMO, 2008).

SunDu has been regarded as a measure of cloud cover as direct radiation is generally lower than 80 W m^{-2} for scattered clouds (cumulus, stratocumulus) (WMO, 2008). High and thin cirrus, as well as aerosols only reduce SunDu at low solar elevations, i.e., at times when the incident clear sky solar radiation is not much larger than 120 W m^{-2}.

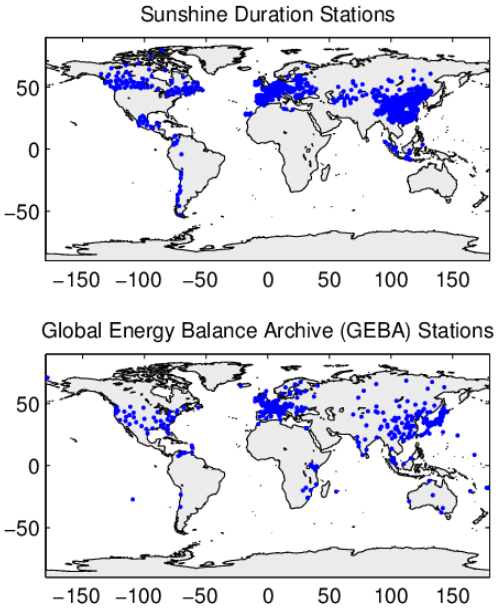

Fig. 1. A map of the Global Energy Balance Archive (GEBA) and Sunshine Duration (SunDu) stations. SunDu data are from the National Climate Data Center (NCDC) Integrated Surface Hourly Database and Chinese SunDu data are obtained from the Chinese Meteorological Administration. Each point in upper pannel represents a SunDu station where more than 120 months of data of SunDu are available (1165 stations in total). Considering the data availability, we divided the stations into six geographic regions: Europe (35–65° N, 10° W–40° E), Iran (20–50° N, 30–55° E), Indonesia (20° S–20° N, 65–130° E), China (20–55° N, 55–150° E), North America (primarily Canada and Mexico, 15–65° N, 160–60° W), and Chile (60° S–15° N, 90–35° W). The number of stations in the regions are 373 (Europe), 26 (Iran), 417 (China), 75 (Indonesia), 119 (Canada and Mexico), and 26 (Chile).

The National Climate Data Center Integrated Surface Hourly Database (Smith et al., 2011) has approximately 4000 stations that reported SunDu from 1982 to 2008. Data durations of about 2200 of these stations exceed one year, and about 1200 stations have more than ten-year data (Fig. 1). We also used SunDu data obtained from the China Meteorological Administration in this study. Most of the data are from the Northern Hemisphere. The Chinese and European datasets have the highest density. All the meterological data used in this paper are also from the Integrated Surface Hourly (ISH) Database released by the National Climate Data Center.

3 Method

The correlation between SunDu and R_s was described by the Ångström formula (Kimball, 1919; Angstrom, 1924) that Prescott subsequently modified (Prescott, 1940). The modified expression assumes a linear relationship between relative R_s and SunDu, and usually results in a good fit. However,

the regression coefficients obtained may only apply to a particular location and not be applicable elsewhere (Sanchez-Lorenzo et al., 2009).

Yang et al. (2006) proposed a physically-based hybrid model to estimate R_s from SunDu. Their hybrid model followed the original Ångström-Prescott model but parameterized radiative extinctions of air and cloud separately. Daily solar radiation (R_s) can be parameterized as (Yang et al., 2006):

$$R_s/R_c = a_0 + a_1 \cdot n/N + a_2 \cdot (n/N)^2 \quad (1)$$

where n is measured SunDu; N is the theoretical values of SunDu and R_c is daily solar radiation under clear-sky conditions. N at a station depends on its location and day of a year. The effect of Rayleigh scattering, water vapor absorption, and ozone absorption, can be accounted for in R_c by using meteorological observations including air temperature and humidity (Yang et al., 2006). The water vapor absorption of solar radiation has been included in the calculation of R_c. This absorption contributed to the reported global dimming (about 1 W m^{-2} in 30 yr) as atmospheric water vapor content increased with global warming (Simmons et al., 2010).

Yang et al. (2006) used winter- and summer-averaged aerosols based on Hess et al. (1998). The inter-annual variation of aerosols was not included. This inter-annual variation can be captured by the observed SunDu (Horseman et al., 2008; Kaiser and Qian, 2002; Raschke et al., 2006; Sanchez-Lorenzo et al., 2008; Sanchez-Lorenzo et al., 2009; Tang et al., 2011). Yang et al. (2006) used one year of SunDu data in Japan and R_s to derive a_0, a_1, and a_2 in Eq. (1) and validated their values based on one year of USA data (1998), one year of Saudi Arabia data (1998), and two years of Chinese data (1997, 1998). For this study, we used long-term measurements from a number of stations to improve parameter estimation.

4 Validation

4.1 Validation data

We used direct measurement of R_s collected by GEBA (Fig. 1) to evaluate that derived from SunDu. Similarly to SunDu, the R_s direct measurements from GEBA have the greatest density over Europe and China with European data quality possibly exceeding data quality over China (Fig. 1, see also Sect. 3.3).

The substantial variation of atmospheric aerosols over Europe and China, from the 1980s to the 2000s (Wang et al., 2009), provided a good test of whether SunDu measurements would accurately characterize these effects on R_s. Therefore, we evaluated Eq. (1) in Europe and China from 1982 to 2005 when both SunDu and GEBA station data were available. 86 stations over Europe and 51 stations over China were selected where GEBA R_s and SunDu data overlap for at least 84 months from 1982 to 2008 (Table 1).

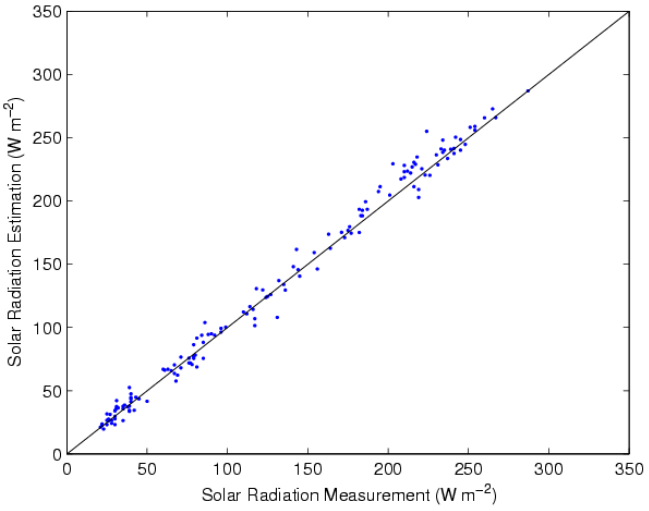

Fig. 2. An example of the comparison between monthly averages of solar radiation (R_s) measurements and our prediction from SunDu at GEBA station No. 1193 (Kucharovice, CZECH REPUBLIC, see Table 1). More information on other stations is available in Table 1.

We used 80 stations, 40 in China and 40 in Europe (bold site name in Table 1), to derive the coefficients, and the other 57 stations to validate them. The derived coefficients of Eq. (1) are $a_0 = 0.33$, $a_1 = 0.70$, and $a_2 = -0.02$, and were used globally for all stations. Both European and Chinese sites were selected to derive and validate the coefficients to show the suitability of Eq. (1) for global usage. Table 1 confirms this by showing that Eq. (1) works well for both development and validation sites and it can be applied globally. Therefore, in the following discussion, we merged all the sites to show their regional variations.

The application of the method for estimating R_s from SunDu depends on answers to the following questions: (a) Can SunDu accurately estimate the extent to which aerosols and cloud properties modify R_s spatially and seasonally? (b) Can SunDu provide reliable estimates of inter-annual and decadal variations of R_s? The following two sections evaluate these two aspects.

4.2 Seasonal variation of R_s

This analysis indicates that this method accurately predicts seasonal variations in R_s. The seasonal variations are primarily determined by solar zenith angle and cloud variations. The overall standard deviation is 12 W m^{-2} (8.6 % in relative value) with a correlation coefficient of 0.98. Figure 2 shows a comparison between GEBA R_s measurements and those derived from SunDu at one station. Table 1 summarizes the comparisons for all stations.

To further test our method, we calculated monthly anomalies in R_s. For each station, we averaged all available R_s data

Table 1. A summary of the locations of the 137 stations in Europe and China where GEBA R_S measurements and estimates from SunDu and aerosol optical depth (AOD) overlap for at least 84 months. The statistical parameters of the comparison between R_S measurements and estimates are shown as standard deviation (STD), bias and averaged R_S in W m^{-2}. To show the capability of the method to quantify the effect of clouds on R_S, the statistical parameters of the comparisons of predicted and measured monthly R_S anomalies (seasonal cycle removed) are also shown. Data at site names in bold were used to calibrate our method and others are used to validate the method.

Station No.	Station Name	Country	Lat (°)	Lon (°)	Monthly R_S			Monthly R_S anomaly		Averaged R_S
					STD	Bias	R	STD	R	
1169	**Innsbruck Univ.**	AUSTRIA	47.27	11.40	14.3	−11.6	0.97	13.4	0.64	128.9
1182	**Sofia**	BULGARIA	42.68	23.33	20.3	15.5	0.97	17.9	0.58	136.8
1188	**Locarno-Monti**	SWITZERLAND	46.17	8.78	13.0	−13.2	0.99	11.0	0.82	147.2
1189	**Hradec Kralove**	CZECH REPUBLIC	50.25	15.85	12.6	−15	0.99	8.7	0.86	120.7
1190	**Ostrava-Poruba**	CZECH REPUBLIC	49.82	18.15	15.2	−8.5	0.98	12.8	0.60	112.2
1191	**Strbske Pleso**	SLOVAKIA	49.12	20.08	12.8	−9.5	0.98	11.2	0.74	122.0
1192	**Churanov**	CZECH REPUBLIC	49.07	13.62	11.5	−8.4	0.99	11.1	0.76	122.1
1193	**Kucharovice**	CZECH REPUBLIC	48.88	16.08	8.6	−3.0	1.00	6.4	0.91	126.6
1195	**Bratislava**	SLOVAKIA	48.17	17.10	11.1	−11.9	0.99	8.2	0.82	134.9
1197	**Potsdam**	GERMANY	52.38	13.10	5.9	−1.4	1.00	5.4	0.96	114.3
1199	**Fichtelberg**	GERMANY	50.43	12.95	23.0	−4.5	0.95	19.3	0.58	110.3
1202	**Norderney**	GERMANY	53.72	7.15	10.6	−11.9	1.00	6.7	0.93	117.6
1203	**Hamburg**	GERMANY	53.65	10.12	6.5	0.8	1.00	6.0	0.96	106.3
1204	**Bremen**	GERMANY	53.05	8.80	7.5	−4.7	0.99	7.2	0.90	107.0
1205	**Braunschweig**	GERMANY	52.30	10.45	5.6	−5.1	1.00	4.9	0.97	115.0
1206	**Osnabrueck**	GERMANY	52.25	8.05	5.5	−5.5	1.00	5.0	0.97	112.0
1207	**Bocholt**	GERMANY	51.83	6.53	6.4	−7.0	1.00	5.9	0.95	116.8
1208	**Bad Lippspringe**	GERMANY	51.78	8.83	6.8	−4.2	1.00	6.3	0.95	109.3
1209	**Braunlage**	GERMANY	51.72	10.62	8.0	−2.4	0.99	7.5	0.92	110.3
1210	**Gelsenkirchen**	GERMANY	51.50	7.08	6.0	0.1	1.00	5.7	0.94	108.3
1211	**Kassel**	GERMANY	51.30	9.45	6.3	−6.0	1.00	5.7	0.95	113.5
1212	**Bonn**	GERMANY	50.70	7.15	7.4	−4.9	0.99	7.3	0.91	113.3
1213	**Giessen**	GERMANY	50.58	8.70	8.0	−5.3	0.99	7.6	0.93	116.0
1214	**Coburg**	GERMANY	50.27	10.95	8.8	−6.8	0.99	8.0	0.92	119.2
1216	**Wuerzburg**	GERMANY	49.77	9.97	8.4	−13.2	1.00	5.9	0.95	125.3
1217	**Trier**	GERMANY	49.75	6.67	9.9	−8.3	1.00	7.6	0.93	121.3
1218	**Mannheim**	GERMANY	49.52	8.55	6.6	−4.3	1.00	6.2	0.95	121.3
1219	**Nuernberg**	GERMANY	49.5	11.08	6.4	−3.8	1.00	6.1	0.96	119.5
1220	**Saarbruecken**	GERMANY	49.22	7.12	9.2	−5.4	0.99	8.7	0.93	119.1
1221	**Weissenburg**	GERMANY	49.02	10.97	7.1	−6.7	1.00	6.7	0.91	124.5
1223	**Passau**	GERMANY	48.58	13.47	6.7	−9.3	1.00	5.6	0.94	126.7
1224	**Weihenstephan**	GERMANY	48.40	11.70	9.3	−11.0	0.99	7.3	0.88	126.6
1225	**Freiburg**	GERMANY	48.00	7.85	17.9	−1.0	0.98	13.2	0.72	129.1
1226	**Hohenpeissenberg**	GERMANY	47.80	11.02	9.6	−16.1	0.99	8.6	0.87	135.4
1228	**Santander**	SPAIN	43.47	−3.82	9.8	−6.2	0.99	8.7	0.82	142.1
1229	**Oviedo**	SPAIN	43.35	−5.87	8.9	−1.5	0.99	8.2	0.85	135.7
1230	**Piikkio**	FINLAND	42.47	−2.40	10.7	−9.4	0.99	9.5	0.77	160.7
1231	**Madrid-Universitaet**	EL SALVADOR	40.45	−3.72	10.1	−8.3	0.99	8.5	0.81	188.9
1233	**Palma de Mallorca**	SPAIN	39.55	2.62	10.0	−9.0	0.99	8.1	0.72	181.1
1234	**Caceres**	SPAIN	39.47	−6.33	9.0	−7.3	0.99	7.4	0.90	195.2
1241	Reims	FRANCE	49.30	4.03	19.9	−21.4	0.97	17.3	0.53	129.9
1242	Caen	FRANCE	49.18	−0.47	20.3	−15.8	0.96	19.1	0.46	129.1
1243	Paris-Montsouris	FRANCE	48.82	2.33	13.7	1.8	0.98	12.7	0.7	109.5
1245	Trappes	FRANCE	48.77	2.02	14.7	−11.9	0.98	12.8	0.66	124.9
1246	Nancy-Essey	FRANCE	48.68	6.22	9.1	−12.2	1.00	7.2	0.92	125.9
1247	Strassburg	FRANCE	48.55	7.63	10.9	−12.9	0.99	8.6	0.86	129.0
1248	Rennes	FRANCE	48.07	−1.73	8.1	−8.8	0.99	7.3	0.89	129.9
1249	Auxerre	FRANCE	47.80	3.55	12.7	−13.8	0.99	8.7	0.84	125.3
1257	Limoges	FRANCE	45.82	1.28	10.1	−6.5	0.99	9.0	0.88	144.5
1258	Clermont-Ferrand	FRANCE	45.78	3.17	8.4	−9.8	0.99	7.7	0.87	144.4
1259	Bordeaux	FRANCE	44.83	−0.70	6.9	−6.8	1.00	6.2	0.91	149.9
1261	Biscarrosse	FRANCE	44.43	−1.25	9.3	−6.7	0.99	8.1	0.84	151.8
1264	Millau	FRANCE	44.12	3.02	25.3	−18.6	0.95	24	0.58	159.4
1266	Nice	FRANCE	43.65	7.20	9.8	−11.8	0.99	7.8	0.81	175.3
1268	Marignane	FRANCE	43.43	5.22	6.0	−10.0	1.00	4.9	0.91	176.7
1274	Ajaccio	FRANCE	41.92	8.80	9.3	−11.0	0.99	8.1	0.77	182.5

Table 1. Continued.

Station No.	Station Name	Country	Lat (°)	Lon (°)	Monthly R_s			Monthly R_s anomaly		Averaged R_s
					STD	Bias	R	STD	R	
1320	Budapest	HUNGARY	47.43	19.18	13.5	−15.3	0.99	11.6	0.65	136.2
1324	Szarvas	HUNGARY	46.87	20.53	17.3	−29.5	0.98	13.8	0.55	146.2
1329	Malin Head,C.	IRELAND	55.37	−7.33	8.0	−10.3	1.00	5.6	0.88	106.7
1331	Clones	IRELAND	54.18	−7.23	9.0	−7.0	0.99	8.4	0.77	102.3
1332	Dublin Airport	IRELAND	53.43	−6.25	7.9	−7.6	0.99	7.5	0.81	110.4
1333	Birr	IRELAND	53.08	−7.88	8.6	−9.2	0.99	8.0	0.80	111.5
1334	Kilkenny	IRELAND	52.67	−7.27	8.4	−9.3	0.99	7.4	0.84	114.2
1379	Eelde	NETHERLANDS	53.13	6.58	8.5	−9.2	0.99	7.6	0.92	109.0
1380	De Kooy	NETHERLANDS	52.92	4.78	15.7	−14.6	0.99	12	0.82	121.2
1381	De Bilt	NETHERLANDS	52.10	5.18	8.8	−7.7	0.99	7.9	0.90	111.1
1382	Vlissingen	NETHERLANDS	51.45	3.60	9.4	−14.3	1.00	6.6	0.92	122.8
1383	Beek/Limburg	NETHERLANDS	50.92	5.77	8.1	−8.6	0.99	7.3	0.92	119.0
1393	Zakopane	POLAND	49.28	19.97	15.8	0.0	0.97	13.0	0.61	113.2
1481	Praha/(Prag-Karlov)	CZECH REPUBLIC	50.07	14.43	8.1	−3.7	0.99	7.8	0.85	114.2
1572	Zuerich-Kloten	SWITZERLAND	47.48	8.53	8.1	−10.2	0.99	7.1	0.91	125.8
2040	**Urumqi**	CHINA	43.78	87.62	12.3	5.7	0.99	9.3	0.73	161.1
2042	**Beijing**	CHINA	39.93	116.28	10.0	8.8	0.99	7.4	0.87	157.9
2043	**Lanzhou**	CHINA	36.05	103.88	10.9	21.3	0.99	8.8	0.8	160.9
2044	**Shanghai**	CHINA	31.4	121.48	14.9	12.6	0.94	13.8	0.78	145.7
2045	**Chengdu**	CHINA	30.67	104.02	9.9	26.7	0.98	8.4	0.84	103.9
2047	**Kunming**	CHINA	25.02	102.68	15.2	9.2	0.93	12.4	0.87	175.2
2048	**Guangzhou**	CHINA	23.13	113.32	16.9	27.1	0.89	12.6	0.80	127.6
2077	Bastia	FRANCE	42.55	9.48	8.1	−10.3	0.99	7.1	0.83	175.2
2108	Saentis	SWITZERLAND	47.25	9.35	17.9	−37	0.96	14.5	0.62	149.7
2109	Payerne SMA	SWITZERLAND	46.82	6.95	7.2	−9.1	1.00	5.6	0.93	134.2
2110	Payerne BSRN	SWITZERLAND	46.82	6.95	11.3	−18.4	1.00	6.4	0.91	137.9
2111	Davos	SWITZERLAND	46.8	9.82	17.1	−30.4	0.97	11.4	0.67	153.1
2112	La Dole	SWITZERLAND	46.43	6.10	20.1	−4.4	0.98	11.6	0.81	133.6
2113	Geneve	SWITZERLAND	46.25	6.13	8.7	−9.1	1.00	7.1	0.90	140.2
2114	Basel	SWITZERLAND	47.55	7.58	11.7	−9.8	0.99	11.1	0.78	130.0
2133	Brest	FRANCE	48.45	−4.42	10.9	−8.1	0.99	10.0	0.84	128.0
2134	Bourges	FRANCE	47.07	2.37	9.6	−13.4	0.99	7.2	0.90	141.4
2471	Marseille/Marignane	FRANCE	43.45	5.23	10.6	−11.0	0.99	9.0	0.78	183.2
2472	Montelimar	FRANCE	44.58	4.73	9.0	−10.0	0.99	6.9	0.87	165.9
2734	**Golmud**	CHINA	36.42	94.90	9.5	1.0	0.99	8.6	0.80	220.4
2739	**Shantou**	CHINA	23.40	116.68	13.4	17.5	0.95	11.0	0.87	157.2
2740	**Nanning**	CHINA	22.82	108.35	19.2	13.3	0.93	16.6	0.76	144.5
2741	**Haikou**	CHINA	20.03	110.35	20.1	23.3	0.92	18.5	0.71	154.6
2742	**Fuzhou**	CHINA	26.08	119.28	19.3	14.8	0.92	16.8	0.73	138.1
2744	**Nanjing**	CHINA	32.00	118.80	11.6	22.8	0.97	9.5	0.88	137.1
2745	**Hefei**	CHINA	31.87	117.23	18.3	21.9	0.92	16.9	0.70	136.2
2746	**Chongqing**	CHINA	29.58	106.47	9.9	27.0	0.98	8.5	0.89	99.3
2747	**Changsha**	CHINA	28.22	112.92	15.8	21.5	0.96	12.9	0.82	126.7
2748	**Guiyang**	CHINA	26.58	106.72	16.4	24.4	0.93	15.3	0.71	111.3
2749	**Guilin**	CHINA	25.32	110.30	21.3	29.4	0.9	18.5	0.62	123.0
2750	**Jinghong**	CHINA	22.00	100.80	19.9	7.6	0.85	16.1	0.59	177.4
2751	**Xi'an**	CHINA	34.30	108.93	16.6	5.8	0.96	15.6	0.72	135.0
2752	**Jinan**	CHINA	36.68	116.98	15.7	21.8	0.96	14.0	0.65	149.1
2753	**Erlianhaote**	CHINA	43.65	111.97	11.6	−10.9	0.99	9.7	0.55	198.0
2754	**Yinchuan**	CHINA	38.48	106.22	10.3	−3.3	0.99	8.4	0.81	189.9
2755	**Taiyuan**	CHINA	37.78	112.55	12.3	8.2	0.98	9.8	0.77	160.6
2756	**Changchun**	CHINA	43.90	125.22	14.4	−3.0	0.97	13.7	0.55	158.7
2757	**Tianjin**	CHINA	39.08	117.07	17.4	7.8	0.95	17.0	0.61	155.0
2759	**Hami**	CHINA	42.82	93.52	10.6	−6.3	0.99	6.9	0.78	196.5
2760	**Xining**	CHINA	36.62	101.77	19.2	18.8	0.94	17.8	0.53	172.1
2761	**Heihe**	CHINA	50.25	127.45	11.1	1.9	0.99	10.1	0.8	141.8
2769	**Altay**	CHINA	47.73	88.08	15.0	0.1	0.99	9.3	0.78	172.4
2771	**Dunhuang**	CHINA	40.15	94.68	13.4	−2.0	0.99	11.0	0.66	202.6
2774	**Nanchang**	CHINA	28.60	115.92	15.7	22.9	0.95	11.5	0.85	135.1
2776	**Hailaer**	CHINA	49.22	119.75	11.1	−2.8	0.99	9.5	0.65	157.2

Table 1. Continued.

Station No.	Station Name	Country	Lat (°)	Lon (°)	Monthly R_s			Monthly R_s anomaly		Averaged R_s
					STD	Bias	R	STD	R	
2780	**Luzhou**	CHINA	28.83	105.43	11.1	29.3	0.98	9.8	0.86	105.9
2781	**Tengchong**	CHINA	25.02	98.50	18.1	5.5	0.83	13.8	0.80	172.6
2782	**Mianyang**	CHINA	31.47	104.68	9.5	16.7	0.98	8.6	0.84	113.6
2787	**Datong**	CHINA	40.1	113.33	14.3	0.3	0.98	13.3	0.54	171.0
2790	**Minqin**	CHINA	38.63	103.08	14.5	5.4	0.98	10.6	0.70	195.1
2791	**Ganzhou**	CHINA	25.85	114.95	14.3	19.1	0.96	10.8	0.85	141.1
2792	**Turpan**	CHINA	42.93	89.20	13.8	3.5	0.99	11.5	0.55	173.5
2801	Yan'an	CHINA	36.60	109.50	12.1	17.9	0.98	10.6	0.82	157.7
2803	Xilinhaote	CHINA	43.95	116.07	11.5	3.7	0.99	8.7	0.74	174.6
2805	Yanji	CHINA	42.83	129.47	15.5	−2.3	0.96	13.0	0.68	146.8
2806	Chaoyang	CHINA	41.55	120.45	10.6	2.7	0.98	9.8	0.67	167.5
2812	Lijiang	CHINA	26.87	100.22	15.1	6.8	0.90	14.0	0.77	193.8
2813	Mengzi	CHINA	23.38	103.38	15.9	10.0	0.90	13.8	0.73	176.0
2838	Weining	CHINA	26.85	104.25	15.6	23.7	0.92	12.0	0.87	149.8
2843	Shanghai (1961–1990)	CHINA	31.17	121.43	14.3	18.7	0.95	11.6	0.84	139.0
2845	Shaoguan	CHINA	24.80	113.60	18.9	35.3	0.93	14.3	0.73	124.3
2846	Zunyi	CHINA	27.68	106.92	12.3	34.4	0.98	8.1	0.89	98.2
2852	Zhaotong	CHINA	27.33	103.75	14.1	8.6	0.96	13.6	0.85	163.2
2867	Wageningen	NETHERLANDS	51.97	5.65	10.0	−4.6	0.99	9.7	0.86	108.1
Average					12.0	−1.0	0.98	10.1	0.80	140.0

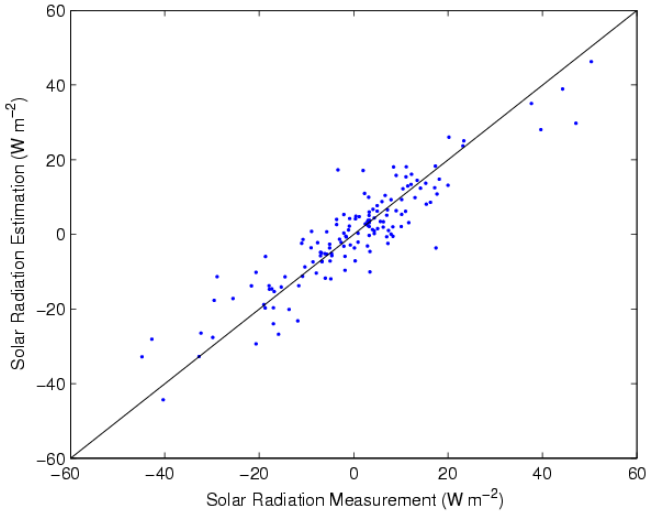

Fig. 3. An example of the comparison between monthly R_s anomalies from direct measurements and our prediction from SunDu at GEBA station No. 1193 (Kucharovice, see Table 1). More information on other stations is available in Table 1.

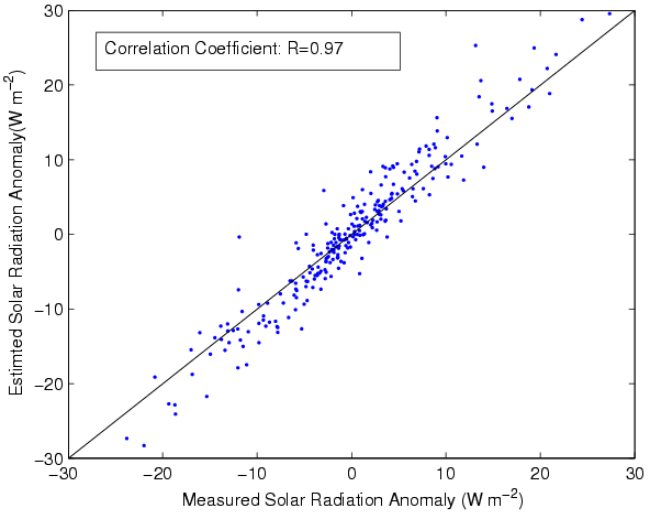

Fig. 4. Comparison between monthly regional R_s anomalies of measurements and our prediction from SunDu. The regional average is over 86 stations in Europe (Table 1). Each point represents one month.

during the study period from 1982 to 2005 for each month. The monthly anomalies were obtained by removing the seasonal cycle from the original monthly R_s data, separately for measured and predicted R_s. Figure 3 illustrates one example of this comparison and all statistical parameters are shown in Table 1, with an overall correlation coefficient of 0.80 averaged from the statistical parameters from each station.

We averaged the anomalies over Europe from all 86 stations, and compared the regional averaged anomalies to the GEBA directly measured values (Fig. 4), and over China from 51 stations (Fig. 5). SunDu-derived R_s also predicts relatively well regional averaged anomalies in R_s and it does a little better over Europe than over China based on regional monthly averages.

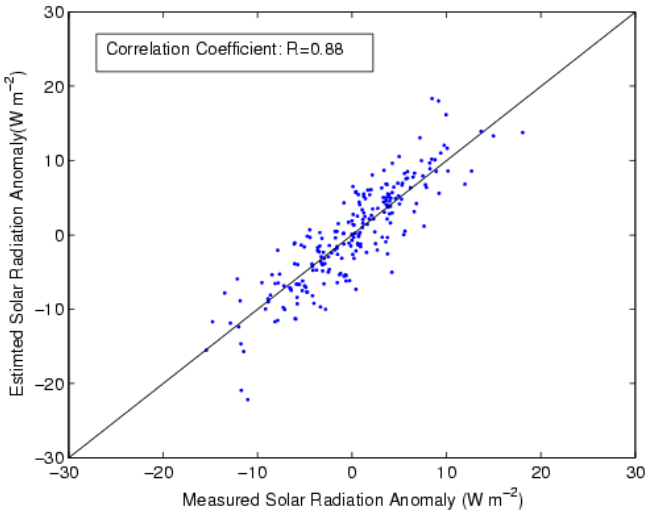

Fig. 5. Comparison between monthly regional R_S anomalies of measurements and our prediction from SunDu. The regional average is over 51 stations in China (Table 1). Each point represents one month.

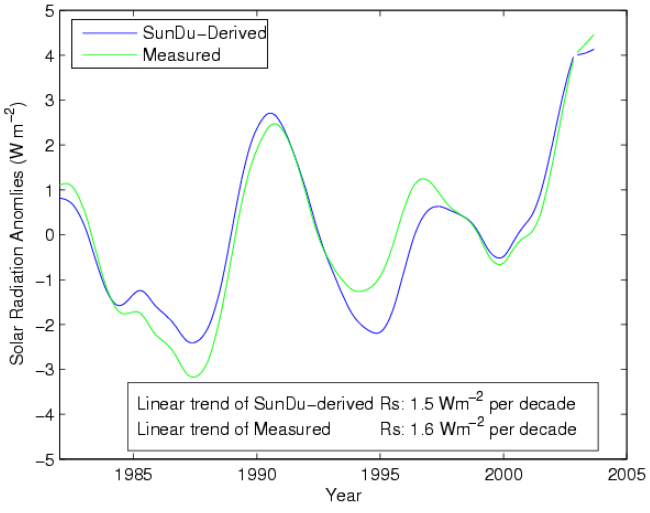

Fig. 6. Comparison of five-year smoothed monthly anomalies of SunDu-derived with directly-measured R_S averaged over 86 stations in Europe (Table 1). The breakpoint in 2003 reflects a break in data availability. The linear trends are calculated annual anomalies rather than five-year smoothed data.

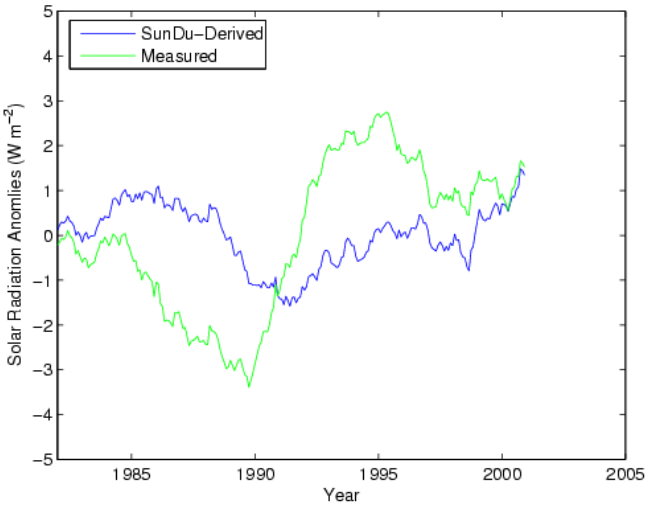

Fig. 7. Comparison of five-year smoothed monthly anomalies of SunDu-derived with directly-measured R_S averaged over 51 stations in China (Table 1). The sharp increase around 1991 in measured R_S occurred when Russian-made pyranometers (Type: DFY) were replaced by Chinese-made pyranometers (Type: TBS) from 1990 to the spring of 1993.

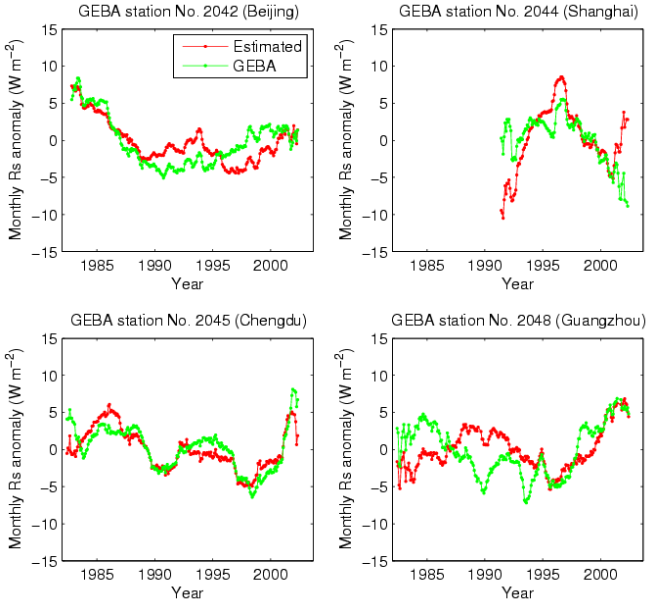

Fig. 8. Comparison between monthly SunDu derived and direct observed R_S at four baseline stations in China.

4.3 Decadal variation of R_S

We also evaluated how well decadal variations in the SunDu-derived R_S are modeled. Figure 6 shows that the decadal variation in R_S is adequately captured by SunDu-derived R_S in Europe. Figure 7 shows that the SunDu-derived R_S also reasonably predicts the variation before 1990 and after 1993 in China. However, there is a sharp increase in the measured R_S between 1990 and 1993 that is not captured by SunDu. Figure 8 shows that SunDu-derived R_S accurately predicts decadal variation in the baseline stations in China, where the pyranometers used to measure R_S were carefully calibrated and maintained. The discontinuity in the other Chinese data (see Fig. 7) occurs during the period from 1990 to the spring of 1993, when China replaced its Russian-made pyranometers (Type: DFY) with Chinese-made pyranometers (Type: TBS) at most stations (CMA, 1996).

Therefore, it appears that the sharp increase in measured R_S was primarily an artifact of instrument replacement and that SunDu-derived R_S can be used to accurately predict decadal variations of R_S in China. The decrease in SunDu-derived R_S in the period of 1990–1992 results from the abrupt increase in stratospheric aerosols (Stevermer et al., 2000) following the Pinatubo volcano eruption in 1991. Further evidence for this conclusion is provided by comparison of both estimates of R_S with pan evaporation. Pan evaporation has been shown to be in good agreement with solar radiation (Roderick and Farquhar, 2002). The variation of pan evaporation from the 1980s to the 2000s in China (Cong et al., 2009) is more strongly correlated with SunDu-derived R_S than the directly-measured R_S shown in Fig. 7. The spuriousness of the discontinuity of R_S direct measurements has also been confirmed by quantify-controlled process studies (Tang et al., 2010, 2011).

In summary, after converting SunDu into R_S using the proposed method (Eq. 1), SunDu-derived R_S agrees very well with direct measurements on inter-annual and decadal time scales.

5 Results

5.1 Inter-annual and decadal variability of regionally averaged R_S

Since SunDu provides a good estimate of R_S and is available in many regions, it can also be used to answer the following questions: (1) How has R_S varied locally and regionally (i.e., 1982 to 2008); and (2) what have been the relative contributions from clouds versus aerosols to the observed variations of R_S?

Decadal variations of R_S around the globe are examined with data from stations that reported SunDu to the World Meteorological Organization, or in China from the Chinese Meteorological Administration. We selected 1165 stations where SunDu and other meteorological data are available for more than 120 months from 1982 to 2008 and divided the sites into six major regions according to their locations and long-term trends (Fig. 1). Daily R_S were calculated and averaged into monthly values for comparison with measurements collected by GEBA.

Figure 9 shows that the R_S derived from SunDu exhibits substantial decadal changes over most regions, similar to those displayed in previous studies (Gilgen et al., 1998; Liepert, 2002; Long et al., 2009; Ohmura, 2009; Stanhill and Cohen, 2001; Wielicki et al., 2002; Wild et al., 2005), and in particular, shows similar variations to those derived from the GEBA. In China, it was flat from the 1990s to 2000 but has been in a pronounced decline since 2000, substantiating the findings of a renewed dimming in China after 2000 (Wild et al., 2009; Xia, 2010).

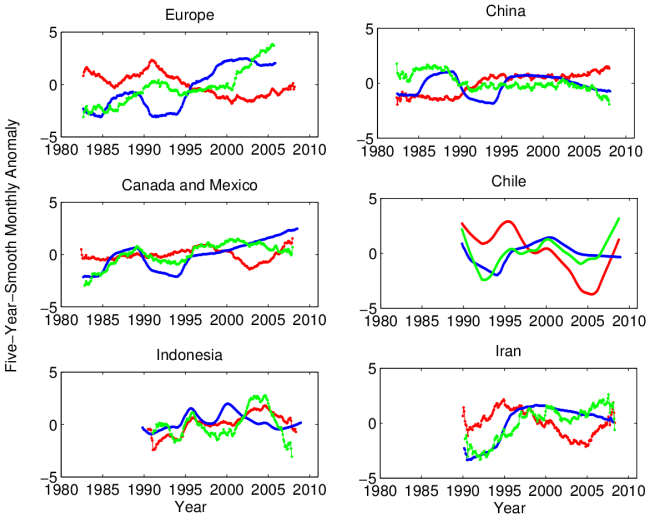

Fig. 9. Five-year smoothed monthly R_S anomalies derived from SunDu as averaged over geographic regions (green line). For comparison, the five-year smoothed clear-sky fraction ($1 - F_C$, red Line) derived from meteorological total cloud fraction measurement (F_C) and negative of column aerosol optical depth (-AOD, blue Line) are also shown. Clear sky fraction and negative AOD are shown here because they are positively correlated with R_S, i.e., both terms imply changes of R_S of the same sign. The 1165 stations are divided into six regions based on the data availability and their trends: **(a)** Europe (35–65° N, 10° W–40° E), **(b)** China (20–55° N, 55–150° E), **(c)** North America (primarily Canada and Mexico, 15–65° N, 160–60° W), **(d)** Chile (60° S–15° N, 90–35° W), **(e)** Indonesia (20° S–20° N, 65–130° E), and **(f)** Iran (20–50° N, 30–55° E).

The sites that measure SunDu in China have a much higher density than those that give direct measurements of R_S (Liang and Xia, 2005; Shi et al., 2008). Furthermore, these SunDu measurements indicate a substantially different decadal variation of R_S over China from the direct measurements (cf., Figs. 9b and 7). Figure 9b shows a substantial decadal variation of R_S occurred in China and Fig. 9e shows that R_S has decreased over Indonesia since 2004.

5.2 Clouds determine R_S at a monthly time scale

We examined the contributions of clouds versus aerosols to the variations of R_S. SunDu has been regarded as a direct measure of cloud cover fraction because all but the thinnest clouds, if intercepting the Sun, will decrease SunDu (Hoyt, 1977). Indeed, as shown in Fig. 10, relative SunDu (the ratio of measured SunDu to maximum possible SunDu during a day) on a monthly scale is highly correlated with ground measured total cloud fraction, i.e., cloud cover variability explains most of the SunDu, and hence R_S variability on inter-annual or shorter time scales.

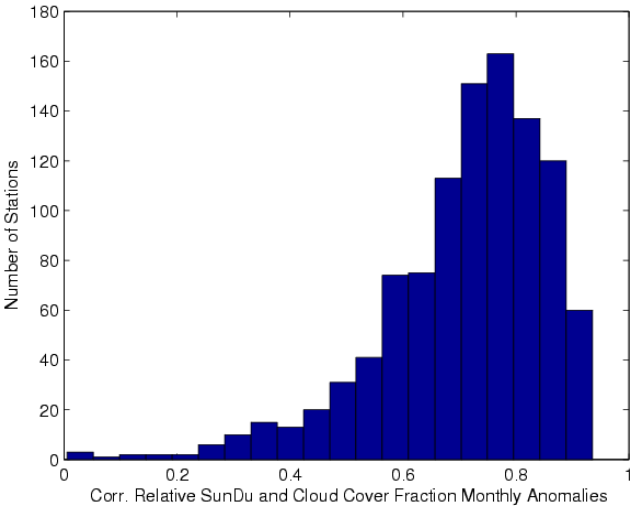

Fig. 10. Histogram of correlations between the relative SunDu (the ratio of measured SunDu to theoretical SunDu during a day) and monthly anomalies of total cloud cover fraction. Total cloud cover fraction is observed visually by trained technicians at weather stations. The plot shows that relative SunDu is highly correlated with cloud cover fraction on a monthly scale at most stations.

5.3 Aerosols contribute most of R_s variability on a decadal time scale

Figure 9 correlates the SunDu-derived R_s with independent data for aerosol optical depth (AOD) as well as cloud cover. The total column AOD is estimated from tropospheric values (Wang et al., 2009) supplemented with satellite-measured stratospheric values (Stevermer et al., 2000). AERONET provides a better dataset of AOD than that derived from visibility (Holben et al., 1998). However, AERONET sites are very sparsely distributed and their data are of short duration. Long-term visibility data are available at most meteorological stations and they have been successfully used to determine long-term variation of tropospheric aerosols from 1973 to 2007 at more than globally 3000 stations (Wang et al., 2009). The clear-sky fraction is obtained from the total cloud cover fraction visually observed at weather stations. Such data from Canada and some countries in Europe have been omitted because of a change in methodology during the 1990's, i.e., surface-cloud observations were changed from human visual to instrumental assessment, resulting in a discontinuity in the data (Dai et al., 2006). Aerosols can only reduce SunDu at low solar elevations. Although, it has been questioned (Stanhill and Cohen, 2005) as to whether SunDu would detect the impact of aerosols on R_s, existing studies have already shown that a reduction in SunDu correlates with increases in atmospheric aerosols (Horseman et al., 2008; Kaiser and Qian, 2002; Qian et al., 2006; Sanchez-Lorenzo et al., 2009).

Figure 9 shows that decadal variability of SunDu-derived R_s is dominated by the changes in aerosols, especially those over Europe and China. The Pinatubo volcanic eruption in 1991 produced a large amount of stratospheric aerosols with substantial anomalies in global AOD and corresponded to a large reduction in R_s in all regions (Fig. 9). The change of cloud cover in Europe compensated the impact of elevated stratospheric aerosols (Fig. 9a). Except during such eruptions, changes in R_s on the decadal time scale are primarily determined by tropospheric AOD anomalies, e.g., the brightening over Europe after 1995, during which time Fig. 9a shows increasing cloud cover but decreasing AOD. Direct concurrent measurements of R_s and AOD (Norris and Wild, 2009; Ruckstuhl et al., 2010) have confirmed that the AOD impact of R_s, i.e., the solar irradiance increase caused by the direct effect of decreasing aerosol, accounts for most of the observed increase of all-sky solar radiation over Europe from 1981 to 2005.

The decline of R_s since 2000 over China (Fig. 9b) was also a result of increased AOD, since cloud cover decreased at that time (Fig. 9b). The substantial increase of AOD in China from the late 1980s to the early 1990s, was compensated by a reduction in cloud cover (Qian et al., 2006; Warren et al., 2007; Xia, 2012) (Fig. 9b). The dips shown in Fig. 9e correspond to all the major fires occurring in Indonesia since 1990 (Podgorny et al., 2003; van der Werf et al., 2008), in particular, the 1991, 1994, 1997–1998 fires, and the reported ramp up of burning after 2000 that culminated in the large fires of 2006 (Podgorny et al., 2003; van der Werf et al., 2008).

The connection between R_s and AOD is further clarified by correlating their five-year smoothed monthly anomalies at each station, i.e., the month-to-month variability seen in Fig. 10 was filtered out. Figure 11 shows that about 58 % percent of all stations with this smoothing have a correlation coefficient larger than 0.5, indicating that the decadal variation in aerosols contributes more than 25 % of the decadal variance in R_s at the majority of the individual stations. Some sites show low correlation or even negative correlation. At the stations, change of clouds is the determining factor of long-term variation of R_s, such as those in the United States (Long et al., 2009).

5.4 Trend of R_s over the Northern Hemisphere

We have merged measurements of R_s derived by SunDu with those directly measured and collected by GEBA. Monthly anomalies were used to obtain a global trend. At each station, its significance was evaluated using the Mann-Kendall test, which is widely used for trend and changing point detection. About 44 % of the stations passed the 95 % confidence test. Figure 12 shows the long-term trends of R_s as aggregated over $5^\circ \times 5^\circ$ grid boxes (302 boxes). The 252 boxes obtained over the Northern Hemisphere have an average trend of $0.87\,\mathrm{W\,m^{-2}}$ per decade. Only 50 boxes were available for R_s data over the Southern Hemisphere and these have a mean trend of zero.

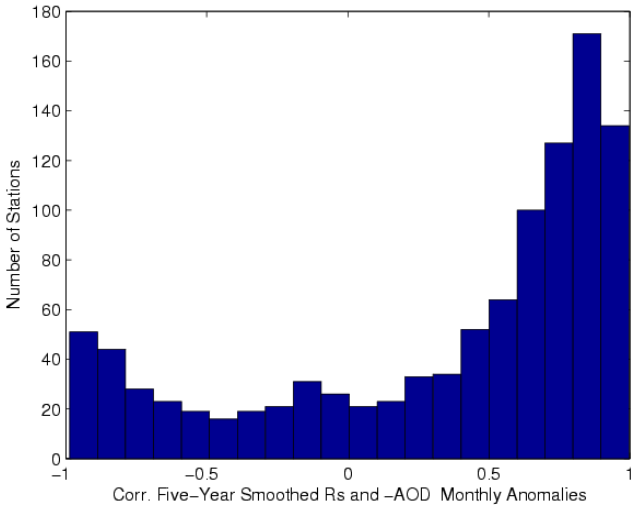

Fig. 11. The histogram of correlations between the five-year smoothed R_S and -AOD monthly anomalies at each station. The five-year (60-month) smoothing filters out high frequency variations in R_S and -AOD (shown in Fig. 10). About 58 % of all stations have a correlation coefficient larger than 0.5. Such correlation coefficients indicate that the decadal variation in aerosols control the decadal variation in R_S (Fig. 9).

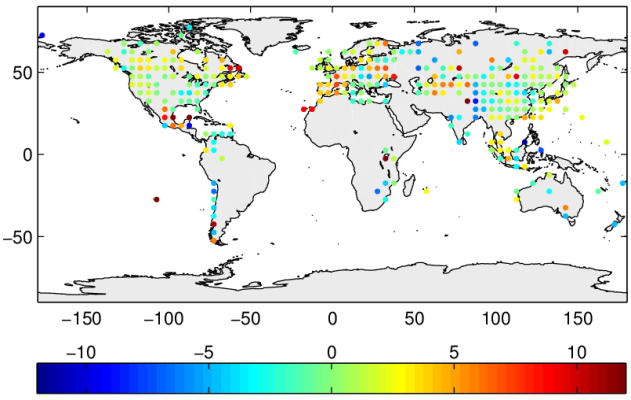

Fig. 12. The linear trend of R_S from 1982 to 2008 (unit: W m^{-2} per decade) from merged SunDu-derived values and direct measurements collected by GEBA. The trends are first calculated at each station and then aggregated into a 5° × 5° grid and the averages are shown. There are 302 such grids obtained and shown.

6 Discussion and conclusions

SunDu is much more widely available and provides a long-term time series dataset where direct measurements are not available, such as in South Asia and South America. Akinoglu (2008) further pointed out that it is the only long term, reliable and readily available measured information that can be used to accurately estimate R_S. Thus, estimation of R_S by SunDu is useful as a complement to globally sparse direct measurements, even in Europe where direct measurements have the highest density. In this study, we investigated the variability of R_S derived by SunDu from 2002 to 2008.

This study shows that SunDu data can describe variations of R_S that are predominantly affected by either cloudiness or aerosols. The SunDu-derived R_S agrees very well with direct measurements on inter-annual and decadal time scales. SunDu as a proxy for R_S provides a stable long-term data series. Compared to its direct measurement, R_S from SunDu appears to be less sensitive to instrument replacement and calibration, and shows that the widely reported sharp increase in R_S during the early 1990s in China was a result of instrument replacement.

The estimates of R_S by SunDu are merged with its direct measurements to provide a long global dataset with high spatial coverage over the Northern Hemisphere. This dataset shows an average increase at a rate of 0.87 W m^{-2} per decade from 1982 to 2008. The average trend over the Southern Hemisphere, whose coverage is much poorer, is negligible. Apparently, the long-term variations of R_S over the two hemispheres are substantially different.

The four major datasets used here, SunDu-derived R_S, satellite-measured stratospheric AOD, visibility-derived tropospheric AOD, and visual observations of cloud cover fraction are totally independent. The consistency of their features show that the conventional SunDu observations supply robust information on atmospheric impact of the climate variability of R_S.

As such, they would be useful to constrain climate model parameterizations that generate R_S variability. Monthly variability of R_S is determined by variability of cloud cover in most regions. The decadal variability of R_S in Europe, China, and North America (primarily Canada and Mexico), is dominated by variations in tropospheric aerosols.

Further analysis would be needed to separate the contributions of direct, indirect, or semi-direct effects of aerosols from the effects of changes in cloud properties. To accomplish this, model simulation would be necessary.

Acknowledgements. The first author was funded by the Global Change Key Research Project (2012CB955302) and National Natural Science Foundation of China (41175126). The second author was funded DOE grant DE-SC0002246, and NSF grant ATM-0720619. The upgrade of the Global Energy Balance Archive has been supported by the Swiss National Competence Center in Climate Research (NCCR climate). The National Climate Data Center Integrated Surface Database (ISD) data were downloaded from (http://www.ncdc.noaa.gov/oa/climate/isd/index.php). We thank G. Stanhill and a anonymous referee for their insightful comments.

Edited by: E. Highwood

References

Angstrom, A.: Solar and terrestrial radiation. Report to the international commission for solar research on actinometric investigations of solar and atmospheric radiation, Q. J. Roy. Meteorol. Soc., 50, 121–126, 1924.

Akinoglu, B. G.: Recent Advances in the Relations between Bright Sunshine Hours and Solar Irradiation, in: Modeling Solar Radiation at the Earth's Surface, edited by: Badescu, V., Springer Berlin Heidelberg, 115–143, 2008.

CMA: Observation method of Meteorological radiation, Meteorological Press, Beijing, 1996.

Cong, Z. T., Yang, D. W., and Ni, G. H.: Does evaporation paradox exist in China?, Hydrol. Earth Syst. Sci., 13, 357–366, doi:10.5194/hess-13-357-2009, 2009.

Dai, A., Karl, T. R., Sun, B., and Trenberth, K. E.: Recent trends in cloudiness over the United States – A tale of monitoring inadequacies, B. Am. Meteorol. Soc., 87, 597–606, 2006.

Essa, K. S. and Etman, S. M.: On the relation between cloud cover amount and sunshine duration, Meteor. Atmos. Phys., 87, 235–240, 2004.

Evan, A. T., Heidinger, A. K., and Vimont, D. J.: Arguments against a physical long-term trend in global ISCCP cloud amounts, Geophys. Res. Lett., 34, L04701, doi:10.1029/2006GL028083, 2007.

Gilgen, H., Wild, M., and Ohmura, A.: Means and trends of shortwave irradiance at the surface estimated from global energy balance archive data, J. Climate, 11, 2042–2061, 1998.

Hayasaka, T., Kawamoto, K., Shi, G. Y., and Ohmura, A.: Importance of aerosols in satellite-derived estimates of surface shortwave irradiance over China, Geophys. Res. Lett., 33, L06802, doi:10.1029/2005GL025093, 2006.

Hess, M., Koepke, P., and Schult, I.: Optical properties of aerosols and clouds: The software package OPAC, B. Am. Meteorol. Soc., 79, 831–844, 1998.

Holben, B. N., Eck, T. F., Slutsker, I., Tanré, D., Buis, J. P., Setzer, A., Vermote, E., Reagan, J. A., Kaufman, Y. J., Nakajima, T., Lavenu, F., Jankowiak, I., and Smirnov, A.: AERONET – a federated instrument network and data archive for aerosol characterization, Remote Sens. Environ., 66, 1–16, 1998.

Horseman, A., MacKenzie, A. R., and Timmis, R.: Using bright sunshine at low-elevation angles to compile an historical record of the effect of aerosol on incoming solar radiation, Atmos. Environ., 42, 7600–7610, 2008.

Hoyt, D. V.: Percent of Possible Sunshine and the Total Cloud Cover, Mon. Weather Rev., 105, 648–652, 1977.

Kaiser, D. P. and Qian, Y.: Decreasing trends in sunshine duration over China for 1954-1998: Indication of increased haze pollution?, Geophys. Res. Lett., 29, 2042, doi:10.1029/2002GL016057, 2002.

Kimball, H. H.: Variations in the total and luminous solar radiation with geographical position in the United States, Mon. Weather Rev., 47, 769–793, doi:10.1175/1520-0493(1919)47<769:vittal>2.0.co;2, 1919.

Liang, F. and Xia, X. A.: Long-term trends in solar radiation and the associated climatic factors over China for 1961–2000, Ann. Geophys., 23, 2425–2432, doi:10.5194/angeo-23-2425-2005, 2005.

Liepert, B. G.: Observed reductions of surface solar radiation at sites in the United States and worldwide from 1961 to 1990, Geophys. Res. Lett., 29, 1421, doi:10.1029/2002GL014910, 2002.

Long, C. N., Dutton, E. G., Augustine, J. A., Wiscombe, W., Wild, M., McFarlane, S. A. and Flynn, C. J.: Significant decadal brightening of downwelling shortwave in the continental United States, J. Geophys. Res., 114, D00D06, doi:10.1029/2008JD011263, 2009.

Norris, J. R. and Wild, M.: Trends in aerosol radiative effects over Europe inferred from observed cloud cover, solar "dimming" and solar "brightening", J. Geophys. Res., 112, D08214, doi:10.1029/2006JD007794, 2007.

Norris, J. R. and Wild, M.: Trends in aerosol radiative effects over China and Japan inferred from observed cloud cover, solar "dimming" and solar "brightening", J. Geophys. Res., 114, D00D15, doi:10.1029/2008JD011378, 2009.

Ohmura, A.: Observed decadal variations in surface solar radiation and their causes, J. Geophys. Res., 114, D00D05, doi:10.1029/2008JD011290, 2009.

Pinker, R. T., Zhang, B., and Dutton, E. G.: Do satellites detect trends in surface solar radiation?, Science, 308, 850–854, 2005.

Podgorny, I. A., Li, F., and Ramanathan, V.: Large Aerosol Radiative Forcing due to the 1997 Indonesian Forest Fire, Geophys. Res. Lett., 30, 1028, doi:10.1029/2002GL015979, 2003.

Prescott, J. A.: Evaporation from water surface in relation to solar radiation, T. Roy. Soc. South Aust., 64, 114–118, 1940.

Qian, Y., Kaiser, D. P., Leung, L. R., and Xu, M.: More frequent cloud-free sky and less surface solar radiation in China from 1955 to 2000, Geophys. Res. Lett., 33, L01812, doi:10.1029/2005GL024586, 2006.

Raschke, E., Bakan, S., and Kinne, S.: An assessment of radiation budget data provided by the ISCCP and GEWEX-SRB, Geophys. Res. Lett., 33, L07812, doi:10.1029/2005GL025503, 2006.

Roderick, M. L. and Farquhar, G. D.: The cause of decreased pan evaporation over the past 50 years, Science, 298, 1410–1411, 2002.

Ruckstuhl, C., Norris, J. R., and Philipona, R.: Is there evidence for an aerosol indirect effect during the recent aerosol optical depth decline in Europe?, J. Geophys. Res., 115, D04204, doi:10.1029/2009JD012867, 2010.

Sanchez-Lorenzo, A. and Wild, M.: Decadal variations in estimated surface solar radiation over Switzerland since the late 19th century, Atmos. Chem. Phys., 12, 8635–8644, doi:10.5194/acp-12-8635-2012, 2012.

Sanchez-Lorenzo, A., Calbo, J., and Martin-Vide, J.: Spatial and Temporal Trends in Sunshine Duration over Western Europe (1938–2004), J. Climate, 21, 6089–6098, 2008.

Sanchez-Lorenzo, A., Calb, J., Brunetti, M. and Deser, C.: Dimming/brightening over the Iberian Peninsula: Trends in sunshine duration and cloud cover and their relations with atmospheric circulation, J. Geophys. Res., 114, D00D09, doi:10.1029/2008JD011394, 2009.

Shi, G. Y., Hayasaka, T., Ohmura, A., Chen, Z. H., Wang, B., Zhao, J. Q., Che, H. Z., and Xu, L.: Data quality assessment and the long-term trend of ground solar radiation in China, J. Appl. Meteorol. Clim., 47, 1006–1016, 2008.

Simmons, A. J., Willett, K. M., Jones, P. D., Thorne, P. W., and Dee, D. P.: Low-frequency variations in surface atmospheric humidity, temperature, and precipitation: Inferences from reanalyses and monthly gridded observational data sets, J. Geophys. Res., 115, D01110, doi:10.1029/2009jd012442, 2010.

Smith, A., Lott, N., and Vose, R.: The Integrated Surface Database Recent Developments and Partnerships, B. Am. Meteorol. Soc., 92, 704–708, 2011.

Stanhill, G. and Cohen, S.: Global dimming: a review of the evidence for a widespread and significant reduction in global radiation with discussion of its probable causes and possible agricultural consequences, Agr. Forest Meteorol., 107, 255–278, 2001.

Stanhill, G. and Cohen, S.: Solar radiation changes in the United States during the Twentieth Century: Evidence from sunshine measurements, J. Climate, 18, 1503–1512, 2005.

Stevermer, A. J., Petropavlovskikh, I. V., Rosen, J. M., and DeLuisi, J. J.: Development of a global stratospheric aerosol climatology: Optical properties and applications for UV, J. Geophys. Res., 105, 22763–22776, 2000.

Tang, W.-J., Yang, K., He, J., and Qin, J.: Quality control and estimation of global solar radiation in China, Sol. Energy, 84, 466–475, 2010.

Tang, W.-J., Yang, K., Qin, J., Cheng, C. C. K., and He, J.: Solar radiation trend across China in recent decades: a revisit with quality-controlled data, Atmos. Chem. Phys., 11, 393–406, doi:10.5194/acp-11-393-2011, 2011.

van der Werf, G. R., Dempewolf, J., Trigg, S. N., Randerson, J. T., Kasibhatla, P. S., Gigliof, L., Murdiyarso, D., Peters, W., Morton, D. C., Collatz, G. J., Dolman, A. J., and DeFries, R. S.: Climate regulation of fire emissions and deforestation in equatorial Asia, P. Natl. Acad. Sci. USA, 105, 20350–20355, 2008.

Wang, K., Dickinson, R. E., and Liang, S.: Clear sky visibility has decreased over land globally from 1973 to 2007, Science, 323, 1468–1470, 2009.

Warren, S. G., Eastman, R. M., and Hahn, C. J.: A survey of changes in cloud cover and cloud types over land from surface observations, 1971–96, J. Climate, 20, 717–738, 2007.

Wielicki, B. A., Wong, T. M., Allan, R. P., Slingo, A., Kiehl, J. T., Soden, B. J., Gordon, C. T., Miller, A. J., Yang, S. K., Randall, D. A., Robertson, F., Susskind, J., and Jacobowitz, H.: Evidence for large decadal variability in the tropical mean radiative energy budget, Science, 295, 841–844, 2002.

Wild, M.: Global dimming and brightening: A review, J. Geophys. Res., 114, D00D16, doi:10.1029/2008JD011470, 2009.

Wild, M., Gilgen, H., Roesch, A., Ohmura, A., Long, C. N., Dutton, E. G., Forgan, B., Kallis, A., Russak, V., and Tsvetkov, A.: From dimming to brightening: Decadal changes in solar radiation at Earth's surface, Science, 308, 847–850, 2005.

Wild, M., Trüssel, B., Ohmura, A., Long, C.N., König-Langlo, G., Dutton, E. G., and Tsvetkov, A.: Global dimming and brightening: An update beyond 2000, J. Geophys. Res., 114, D00D13, doi:10.1029/2008JD011382, 2009.

WMO: Measurement of sunshine duration, WMO guide to meteorological instruments and methods of observation manual on the global observing system, WMO, http://www.wmo.int/pages/prog/gcos/documents/gruanmanuals/CIMO/CIMO_Guide-7th_Edition-2008.pdf (last access: October 2012), 2008.

Xia, X.: A closer looking at dimming and brightening in China during 1961–2005, Ann. Geophys., 28, 1121–1132, doi:10.5194/angeo-28-1121-2010, 2010.

Xia, X.: Significant decreasing cloud cover during 1954–2005 due to more clear-sky days and less overcast days in China and its relation to aerosol, Ann. Geophys., 30, 573–582, doi:10.5194/angeo-30-573-2012, 2012.

Xia, X. A., Wang, P. C., Chen, H. B., and Liang, F.: Analysis of downwelling surface solar radiation in China from National Centers for Environmental Prediction reanalysis, satellite estimates, and surface observations, J. Geophys. Res., 111, D09103, doi:10.1029/2005JD006405, 2006.

Yang, K., Koike, T., and Ye, B. S.: Improving estimation of hourly, daily, and monthly solar radiation by importing global data sets, Agr. Forest Meteorol., 137, 43–55, 2006.